NLRP3 Controls the Development of Gastrointestinal CD11b+ Dendritic Cells in the Steady State and during Chronic Bacterial Infection

Arnold, Isabelle C ; Zhang, Xiaozhou ; Urban, Sabine ; Artola-Borán, Mariela ; Manz, Markus G ; Ottemann, Karen M ; Müller, Anne

Abstract: The gastric lamina propria is largely uncharted immunological territory. Here we describe the evolution and composition of the gastric, small intestinal, and colonic lamina propria mononuclear phagocyte system during the steady state and infection with the gastric pathogen Helicobacter pylori. We show that monocytes, CX3CR1hi macrophages, and CD11b+ dendritic cells are recruited to the infected stomach in a CCR2-dependent manner. All three populations, but not BATF3-dependent CD103+ DCs, sample red fluorescent protein (RFP)+Helicobacter pylori (H. pylori). Mice reconstituted with human hematopoietic stem cells recapitulate several features of the myeloid cell-H. pylori interaction. The differentiation in and/or recruitment to gastrointestinal, lung, and lymphoid tissues of CD11b+ DCs requires NLRP3, but not apoptosis-associated speck-like protein containing a carboxy-terminal CARD (ASC) or caspase-1, during steady-state and chronic infection. NLRP3-/- mice fail to generate Treg responses to H. pylori and control the infection more effectively than wild-type mice. The results demonstrate a non-canonical inflammasome-independent function of NLRP3 in DC development and immune regulation.

DOI: https://doi.org/10.1016/j.celrep.2017.12.015

Article

Cell Reports

NLRP3 Controls the Development of Gastrointestinal CD11b$^+$ Dendritic Cells in the Steady State and during Chronic Bacterial Infection

Graphical Abstract

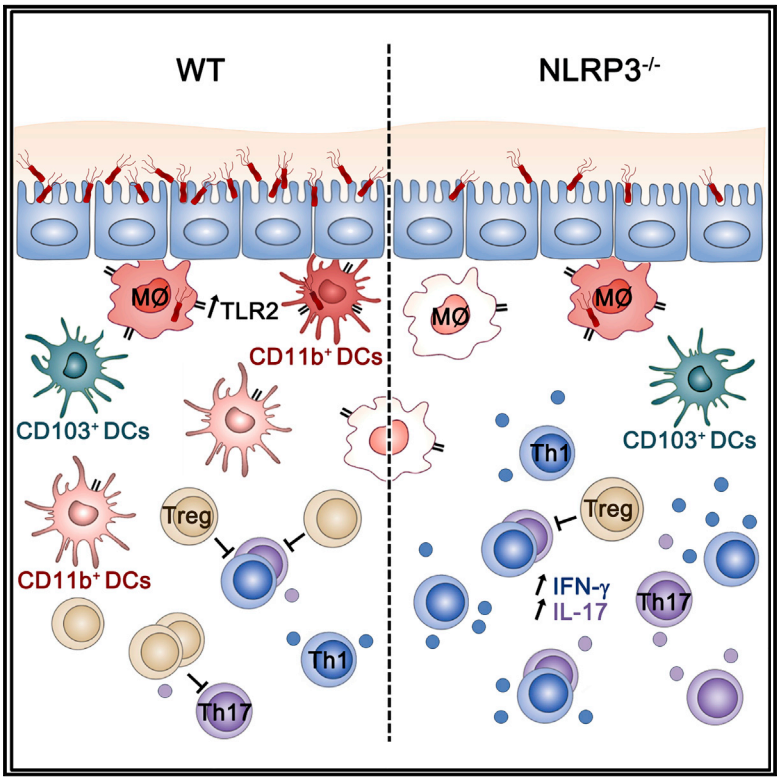

Highlights

- Gastric lamina propria CX_3CR1^{hi} macrophages and CD11b$^+$ DCs sample RFP$^+$ *H. pylori*
- Humanized mice are useful models for studying the phagocyte/*H. pylori* interaction
- NLRP3 is required for the development of CD11b$^+$ DCs but not CD103$^+$ DCs
- NLRP3 is required for Treg development and suppression of Th1 responses

Authors

Isabelle C. Arnold, Xiaozhou Zhang, Sabine Urban, Mariela Artola-Borán, Markus G. Manz, Karen M. Ottemann, Anne Müller

Correspondence

arnold@imcr.uzh.ch (I.C.A.), mueller@imcr.uzh.ch (A.M.)

In Brief

Arnold et al. report that the gastric pathogen *Helicobacter pylori* is sampled by CD11b$^+$ cDC2 dendritic cells that require NLRP3, but not other inflammasome components, for their differentiation in gastrointestinal tissues. NLRP3 deficiency is further associated with loss of regulatory T cells and corresponding dysregulated Th1 responses.

Arnold et al., 2017, Cell Reports *21*, 3860–3872
December 26, 2017
https://doi.org/10.1016/j.celrep.2017.12.015

CellPress

OPEN ACCESS
CellPress

Cell Reports
Article

NLRP3 Controls the Development of Gastrointestinal CD11b$^+$ Dendritic Cells in the Steady State and during Chronic Bacterial Infection

Isabelle C. Arnold,[1,*] Xiaozhou Zhang,[1] Sabine Urban,[1] Mariela Artola-Borán,[1] Markus G. Manz,[2] Karen M. Ottemann,[3] and Anne Müller[1,4,*]

[1]Institute of Molecular Cancer Research
[2]Department of Hematology
University of Zürich, 8057 Zürich, Switzerland
[3]Department of Microbiology and Environmental Toxicology, University of California, Santa Cruz, Santa Cruz, CA, USA
[4]Lead Contact
*Correspondence: arnold@imcr.uzh.ch (I.C.A.), mueller@imcr.uzh.ch (A.M.)
https://doi.org/10.1016/j.celrep.2017.12.015

SUMMARY

The gastric lamina propria is largely uncharted immunological territory. Here we describe the evolution and composition of the gastric, small intestinal, and colonic lamina propria mononuclear phagocyte system during the steady state and infection with the gastric pathogen *Helicobacter pylori*. We show that monocytes, CX_3CR1^{hi} macrophages, and CD11b$^+$ dendritic cells are recruited to the infected stomach in a CCR2-dependent manner. All three populations, but not BATF3-dependent CD103$^+$ DCs, sample red fluorescent protein (RFP)$^+$ *Helicobacter pylori* (*H. pylori*). Mice reconstituted with human hematopoietic stem cells recapitulate several features of the myeloid cell-*H. pylori* interaction. The differentiation in and/or recruitment to gastrointestinal, lung, and lymphoid tissues of CD11b$^+$ DCs requires NLRP3, but not apoptosis-associated speck-like protein containing a carboxy-terminal CARD (ASC) or caspase-1, during steady-state and chronic infection. NLRP3$^{-/-}$ mice fail to generate Treg responses to *H. pylori* and control the infection more effectively than wild-type mice. The results demonstrate a non-canonical inflammasome-independent function of NLRP3 in DC development and immune regulation.

INTRODUCTION

Mononuclear phagocytes (MPs) residing in the lamina propria (LP) of the gastrointestinal (GI) tract contribute critically to the control of invading pathogens and the development of immunity as well as the induction and maintenance of immune tolerance. Specialized subsets of MPs perform distinct and complementary functions in immunity and GI homeostasis; the MP composition differs in the lower and upper GI compartments in the steady state and during inflammation (Cerovic et al., 2014; Lavin et al., 2015; Mowat and Agace, 2014). Although the MP subsets of the small intestine and colon have been studied in detail in terms of their ontogeny, expression of surface markers and lineage-defining transcription factors, and functional specialization, little is known about MPs residing in the gastric LP. In the intestines, MPs are broadly identified either as resident (non-migratory) macrophages that are replenished from blood-derived Ly6C^{hi} monocytes and detect, engulf, and neutralize pathogens and thus exert important innate effector functions or as dendritic cells (DCs). GI tract DCs originate from a pre-DC progenitor, require FLT3L for their development, migrate from mucosal tissues to draining lymph nodes via the lymph, and possess the unique ability to prime the differentiation and polarization of effector cells from naive T cells (Cerovic et al., 2014; Lavin et al., 2015). Intestinal LP macrophages exhibit high surface expression of the chemokine CX_3C receptor (CX_3CR) 1 as well as of F4/80 and CD64 but lack CD103. Intestinal DCs can be divided into at least two distinct lineages depending on their surface marker expression and dependence on transcription and growth factors. CD103$^+$ DCs that additionally express CD11b depend on granulocyte macrophage colony-stimulating factor (GM-CSF) (Greter et al., 2012; Kingston et al., 2009) as well as the transcription factors Notch-2 (Lewis et al., 2011) and IRF4 (Persson et al., 2013) for development. CD103$^+$CD11b$^-$ DCs, in contrast, require the basic leucine zipper transcription factor ATF-like (BATF) 3 and IRF8 (Edelson et al., 2010). Both LP DC subsets, which are now commonly referred to as cDC1 (BATF3/IRF8-dependent) and cDC2 (IRF4/Notch-2-dependent), have lymph node counterparts in the form of CD11b$^+$ and CD8α^+ DCs that share the reliance on IRF4/Notch-2 and IRF8/BATF3, respectively. Functionally, IRF8/BATF3-dependent populations are endowed with a superior ability to cross-present viral, tumor, and self-antigens and have a human functional equivalent in the CD141^{hi} DC subset (Haniffa et al., 2012), whereas IRF4/Notch-2-dependent DCs (likely human equivalent: CD1c$^+$ DCs) have been implicated in Th17 priming (Lewis et al., 2011; Persson et al., 2013). An additional DC subset of the GI LP that is less well understood in terms of its ontogeny expresses IRF4 and CD11b, but neither CD103 nor macrophage markers, and intermediate levels of CX_3CR1; this population is responsive to Flt3L *in vivo*, but its progenitor is controversial (Bain et al., 2013; Cerovic et al., 2013; Scott et al., 2015).

We have reported previously that *Helicobacter pylori*, a pathobiont that colonizes the human gastric mucosa of half of the

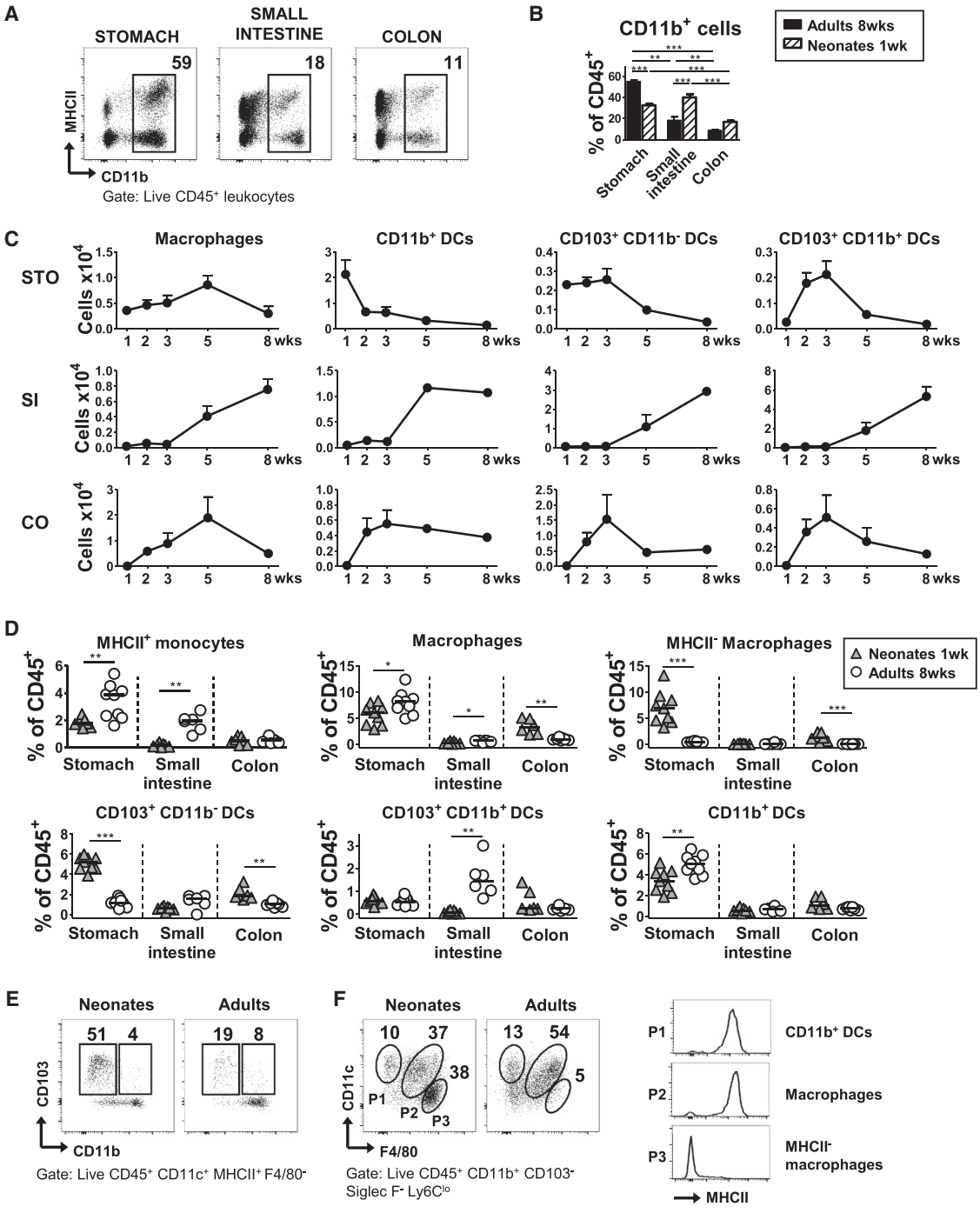

Figure 1. Comparative Analysis of the Evolution and Composition of the Gastric, Small Intestinal, and Colonic LP MP Populations in the Steady State

The indicated MP subsets were isolated from the LP of the stomach, SI, and colon at the indicated age and analyzed by flow cytometry.

(A) Representative FACS plots of CD11b$^+$ myeloid cells in the stomach, SI, and colon, in percent of live CD45$^+$ leukocytes.

(B) Frequencies of CD11b$^+$ myeloid cells in the three compartments in adult (8-week-old) and neonatal (1-week-old) mice. Pooled data from 2 studies are shown (n = 5–9 mice per group). One-way ANOVA was used for statistical analyses. Data are represented as mean + SEM.

(C) Absolute counts per organ of macrophages and of CD11b$^+$, CD103$^+$, and CD103$^+$CD11b$^+$ DCs at the indicated ages. Pooled data from 2 studies are shown (n = 3–5 mice per time point). STO, stomach, SI, small intestine, CO, colon. Data are represented as mean + SEM.

(legend continued on next page)

world's population and is tightly associated with gastric disorders such as ulcers, chronic gastritis, and gastric cancer (Salama et al., 2013), has a major effect on the functionality of DCs (Koch et al., 2015; Oertli et al., 2012, 2013). *Helicobacter pylori* (*H. pylori*) causes a persistent mucosa-associated but non-invasive infection that is characterized by either regulatory T cell (Treg)- or Th1/Th17-predominant responses: in children and neonatally infected mice, the *H. pylori*/host interaction is generally asymptomatic and characterized by a lack of effector T cell responses, predominance of Tregs, and high level colonization (Arnold et al., 2011b; Harris et al., 2008). In contrast, infected adults (especially those presenting with *H. pylori*-associated peptic ulcers) and mice infected as adults exhibit a striking T cell infiltrate that is dominated by effector T cells and limits the bacterial burden without clearing *H. pylori* completely (Arnold et al., 2011b; Harris et al., 2008). Rather, the large quantities of interferon γ (IFN-γ) produced by *H. pylori*-specific Th1 cells are believed to be the direct cause of the pre-malignant lesions—i.e., epithelial hyperplasia and intestinal metaplasia—that precede the development of gastric cancer (Arnold et al., 2011b). The benign interaction of *H. pylori* with its host that is characteristic of pediatric populations has been linked to protective effects against allergic asthma, other forms of allergy, and inflammatory bowel diseases in large epidemiological studies conducted in multiple areas of the world (Blaser et al., 2008; Castano-Rodriguez et al., 2017; Zhou et al., 2013). Several studies have confirmed a protective effect of *H. pylori* in experimental models of allergic asthma induced by ovalbumin (Arnold et al., 2011a) and house dust mite extract (Koch et al., 2015) and in models of sodium dextran sulfate (DSS)-induced colitis (Engler et al., 2015). The protection against allergy was functionally linked to *H. pylori*-induced Tregs and further required the TLR2/NLRP3/caspase-1/interleukin-18 (IL-18) axis because mice lacking any one of these factors failed to develop *H. pylori*-induced immune tolerance (Engler et al., 2015; Koch et al., 2015; Oertli et al., 2012).

Here we have conducted a detailed comparative analysis of the gastric (and small intestinal and colonic) MP populations in the steady state and during *H. pylori* infection to dissect which subsets encounter and sample *H. pylori* and are required for immunity on one hand or homeostasis in the face of infection on the other. We find that gastric MP populations evolve continuously in the first weeks of life and bear more similarities to the colon than to the small intestine. Various MP subsets are recruited to the *H. pylori*-infected mucosa in a CCL2/CCR2-dependent manner, but only monocytes, $CX_3CR1^{dim}CD11b^+$ DCs, and CX_3CR1^{hi} macrophages encounter red fluorescent protein $(RFP)^+$ *H. pylori*. The same cells upregulate TLR2 and NLRP3 upon contact with *H. pylori*. NLRP3, but not other inflammasome components, is required for the differentiation and/or recruitment of $CD11b^+$ DCs during *H. pylori* infection and in the steady state.

RESULTS

The Gastric LP Is Populated by a Myeloid Cell Network that Evolves and Stabilizes in the First Weeks of Life

Because little is known about MP populations of the murine gastric LP, their evolution from early life to adulthood, and their functional specialization during homeostasis and bacterial infection, we performed a detailed parallel analysis of the gastric, small intestinal, and colonic LP compartment by multicolor flow cytometry (Figures S1A and S1B). Although the overall leukocyte population was much smaller in the stomach than in the small and large intestine (Figure S1C), the frequency of myeloid cells, as defined by their expression of CD11b with or without co-expression of major histocompatibility complex (MHC) class II, was substantially higher; whereas >50% of gastric LP leukocytes are of myeloid origin, this figure is as low as 10%–20% in the intestines (Figures 1A and 1B). Interestingly, the MP compartment of neonatal mice (analyzed on day 7 of age) differs strongly from that of adults (age 8 weeks) in all three organs and appears to be more homogeneous across organs in newborns (Figure 1B). A more detailed inspection revealed highly divergent patterns of myeloid evolution in the three organs during the first 2 months of life (Figures 1C–1F and S1C). Several interesting parallels were observed between the colon and stomach that were not shared by the small intestine (SI); in particular, macrophage and $CD103^+$ $CD11b^+$ DC populations increase steadily in the first weeks of life and contract again at or just after weaning (Figure 1C). In contrast to the adult SI, where $CD103^+$ $CD11b^+$ DCs represent the numerically dominant MP population by far, this population is relatively minor in both the adult stomach and colon in the steady state (Figures 1C and 1D). Further, the stomach and colon are populated in neonates by large numbers and/or high frequencies of $CD11b^+$ DCs, $CD103^+$ DCs, and MHC class II-negative macrophages, which disappear or are reduced within the first 2 weeks of life and, thereafter, are replaced by MHC class II-positive monocytes and macrophages (Figures 1C–1F and S1D). In summary, the gastric LP is a predominantly myeloid cell-populated organ and devoid of lymphocytes in the steady state; the observed patterns of myeloid evolution indicate that adult-predominant myeloid lineages replace neonatal DC and macrophage lineages at approximately the time of weaning.

Experimental Infection with *H. pylori* Triggers the CCR2-Dependent Gastric Recruitment of Various MPs Required for T Cell-Mediated Infection Control

To examine how a challenge infection with the common gastric pathobiont *H. pylori* would affect the gastric LP compartment, we infected 6-week-old mice with a mouse-colonizing human isolate of *H. pylori* and quantified the myeloid and lymphoid populations at 1 and 3 months post infection. Exposure to *H. pylori*

(D) Frequencies of the indicated MP populations, as assessed at 1 and 8 weeks of age. Horizontal lines indicate medians. *$p < 0.05$, **$p < 0.01$, ***$p < 0.001$, as calculated by Mann-Whitney test. Data are pooled from 2 independent studies (n = 5–9 mice per group); note that somewhat fewer SI samples were prepared than of the other two organs because of the technical challenges posed by this organ.

(E and F) Representative FACS plots of DC subsets (E), macrophages, and $CD11b^+$ DCs (F) in 1-week-old (neonate) and 8-week-old (adult) mice. The histograms at the right show the MHC class II expression of macrophages and $CD11b^+$ DCs.

See also Figure S1.

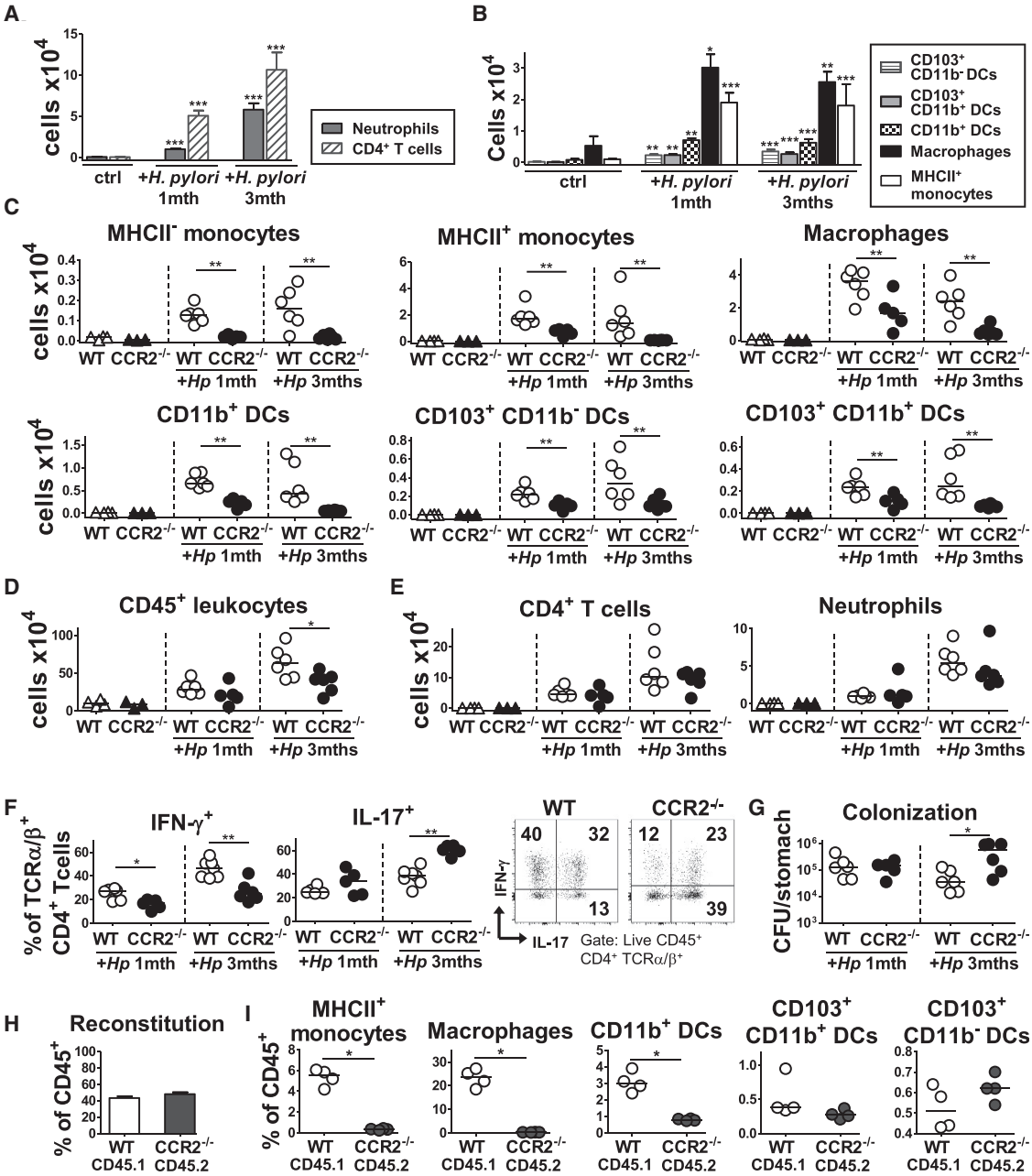

Figure 2. Cell-Intrinsic Dependence of Monocytes, Macrophages, and CD11b$^+$ DCs on CCR2 for Recruitment to the Gastric LP

(A and B) Absolute counts of neutrophils and CD4$^+$ T cells (A) and of various MP populations (B) in the LP of mice in the steady state and at 1 and 3 months post infection (p.i.) with *H. pylori*. Data are represented as mean + SEM. One representative study of 2 is shown; n = 2–4 mice per group. The p values were calculated relative to uninfected controls by one-way ANOVA with Bonferroni post-test.

(C) Absolute counts of the indicated gastric LP MP populations in WT and CCR2$^{-/-}$ mice in the steady state and at 1 and 3 months p.i. with *H. pylori*.

(D–F) Absolute counts of all leukocytes (D) and CD4$^+$ T cells and neutrophils (E) and frequencies of IFN-γ$^+$ and IL-17$^+$ CD4$^+$ T cells (F) in the gastric LP of WT and CCR2$^{-/-}$ mice in the steady state and at 1 and 3 months p.i. with *H. pylori*. In (F), representative FACS plots are shown as well.

(G) *H. pylori* colonization of the mice shown in (A–F), represented as CFUs per stomach.

(H and I) Adult WT mice were reconstituted with 1:1 mixed bone marrow from CD45.1$^+$ WT and CD45.2$^+$ CCR2$^{-/-}$ donors. Mice were allowed to reconstitute for 6 weeks prior to a 6-week infection with *H. pylori*. The reconstitution efficiency in percent of all CD45$^+$ cells is shown in (H). The frequencies of the indicated MP populations are shown in (I) (n = 4 mice per group).

The data in (C–G) are representative of 2 independently conducted time courses (n = 3–6 mice per group). In (C–G) and (I), horizontal lines indicate medians. *p < 0.05, **p < 0.01, ***p < 0.001, as calculated by Mann-Whitney test. See also Figure S2.

triggered a robust influx into the gastric LP of neutrophils and $CD4^+$ T cells; these populations were numerically dominant and increased progressively over time (Figure 2A). $CD103^+$ DCs, $CD103^+CD11b^+$ DCs, $CD11b^+$ DCs, macrophages, and monocytes were recruited as well but reached a plateau already 1 month post infection (Figure 2B). The recruitment of MHC class II^+ and MHC class II^- monocytes and of macrophages and DC lineages to the chronically infected stomach depended strongly on the CCL2/CCR2 chemokine/receptor axis as CCR2-deficient animals exhibited a clear defect in the recruitment of all MP lineages (Figure 2C) that was also reflected in the overall leukocyte counts at 3 months post infection (p.i.) (Figure 2D); in contrast, the recruitment of neutrophils and $CD4^+$ T cells was unaffected by CCR2 deficiency (Figure 2E). In wild-type mice, LP T cells exhibited a clear polarization toward both Th1 and Th17 lineages, with >70% of all T cells producing the lineage-specific signature cytokines IFN-γ or IL-17 (or both; Figure 2F). In contrast to wild-type mice, CCR2-deficient animals exhibited reduced frequencies of Th1 cells, but not of Th17 cells, and failed to control the infection at the 3-month time point (Figures 2F and 2G). We next generated mixed bone marrow chimeras to examine which MP populations require cell-intrinsic CCR2 signaling for gastric LP recruitment during infection. Interestingly, monocytes, macrophages, and $CD11b^+$ DCs (which we consider to be *bona fide* DCs because they are absent in the gastric LP of infected $FLT3L^{-/-}$ mice; Figure S2), but not $CD103^+$ DC lineages, failed to migrate to the infected stomach in this setting (Figures 2H and 2I). The combined results suggest that gastric MP populations can be divided into cell-intrinsically CCR2-dependent phagocytes ($CD11b^+$ DCs, macrophages, and monocytes) and those that are only indirectly dependent on CCR2 ($CD103^+$ DCs). MP recruitment to the gastric mucosa, in turn, is associated with proper Th1 activation and *H. pylori* control.

CX_3CR1^{hi} Macrophages and $CD11b^+$ DCs Sample *H. pylori* in the Murine Gastric Mucosa

To address which of the MP cells that may potentially encounter *H. pylori* in the gastric mucosa phagocytose and sample the bacteria, we generated mouse-colonizing *H. pylori* strains expressing either GFP or RFP. Both fluorescent proteins were expressed, could be detected by fluorescence-activated cell sorting (FACS) in cultured bone marrow-derived phagocytes, and were stable intracellularly for up to 48 hr after phagocytosis (data not shown). The RFP signal proved to be more stable over time than the GFP signal, and, therefore, RFP^+ *H. pylori* was used in all subsequent *in vivo* experimentation. Not surprisingly, the detection of RFP signal in LP cells was most straightforward in mice with high levels of colonization. To achieve this, we infected mice neonatally (i.e., on day 6 or 7 of age) at a time when the animals develop immune tolerance rather than immunity to the infection (Arnold et al., 2011b). In adult mice that had been infected neonatally, around 4% of the myeloid $CD11b^+$ population exhibited an RFP signal (Figure 3A). The RFP signal could further be tracked to MHC class II^+ monocytes, macrophages, and $CD11b^+$ DCs but was largely absent in the two other DC subsets (Figures 3B and 3C). Infection of *CX_3CR1*-GFP reporter mice, in which GFP is expressed in all CX_3CR1-positive cells, confirmed that the RFP signal was restricted to *CX_3CR1*-GFP^{hi} $F4/80^{hi}$ macrophages, $CD11b^+$ CX_3CR1^{dim} $F4/80^-$ DCs, and CX_3CR1^{dim} monocytes (Figure 3D; data not shown). A similar distribution of RFP signal, albeit at a generally lower frequency, was observed in animals that had been infected as adults and, therefore, had a significantly lower bacterial burden (Figures S3A and S3B). No RFP signal was detectable in mesenteric lymph node (MLN) preparations despite numerous attempts to track the signal within migrating antigen presenting cells (APCs). The combined results indicate that CX_3CR1-positive macrophage, monocyte, and DC populations, but not $CD103^+$ DCs, phagocytose *H. pylori* in the gastric mucosa.

RFP^+ *H. pylori* Is Phagocytosed by Human Monocytes and Macrophages in Mice with Reconstituted Human Immune Systems

We next established a humanized mouse model of *H. pylori* infection to assess which human myeloid cells sample RFP^+ bacteria. Non-obese diabetic (NOD)/LtSz-scid IL2Rγ deficient (NSG) mice reconstituted at birth with human $CD34^+$ cord blood cells proved to be insufficiently permissive to myeloid cell development and, rather, favored lymphoid engraftment both in the spleen and the GI tract LP (data not shown). We instead took advantage of "MISTRG" mice, which express several human cytokines central to myeloid development and hematopoietic stem cell maintenance (macrophage colony stimulating factor [M-CSF], IL-3, GM-CSF, and thrombopoietin) under their endogenous promoters, as well as human SIRPα as a transgene, on a Rag2-deficient, Il2Rγ-deficient background (Rongvaux et al., 2014). MISTRG mice are superior to NSG mice in terms of their myeloid cell engraftment in bone marrow and spleen and the full recapitulation of human myeloid development and function (Rongvaux et al., 2014). In the gastric LP of MISTRG mice, the frequency of $hCD45^+$ cells was low, at <1% of all live cells, but roughly doubled upon infection with *H. pylori* (Figure 3E). The increase due to infection could be attributed to an influx of $CD14^+CD16^+$ monocytes (Figure 3F). A second population of myeloid cells, $CD163^+$ macrophages, was already present in the gastric LP in the steady state and did not change upon infection (Figure 3G). Both populations exhibited a clearly discernible RFP signal in, on average, 4% and 11% of the population upon infection (Figure 3H), suggesting that human mononuclear phagocytes indeed develop normally and acquire comparable effector functions in murine hosts. Although two major human DC populations, $CD1c^+$ DCs and $CD141^+$ DCs, were detectable in the gastric LP, their numbers and frequencies were so low (under 2%) that detecting RFP signals in these populations was impossible. Furthermore, we found no evidence of increased LP T cell frequencies in infected mice and also could not detect differences in colonization levels in reconstituted relative to non-reconstituted MISTRG mice (Figure 3I and data not shown). In summary, MISTRG mice are more permissive to human myeloid cell engraftment in the gastric LP than NSG mice and, therefore, can be used to investigate human myeloid cell responses to *H. pylori* infection in an *in vivo* setting; the recruitment of phagocytes to the infected mucosa and their sampling of *H. pylori* indicate that innate human

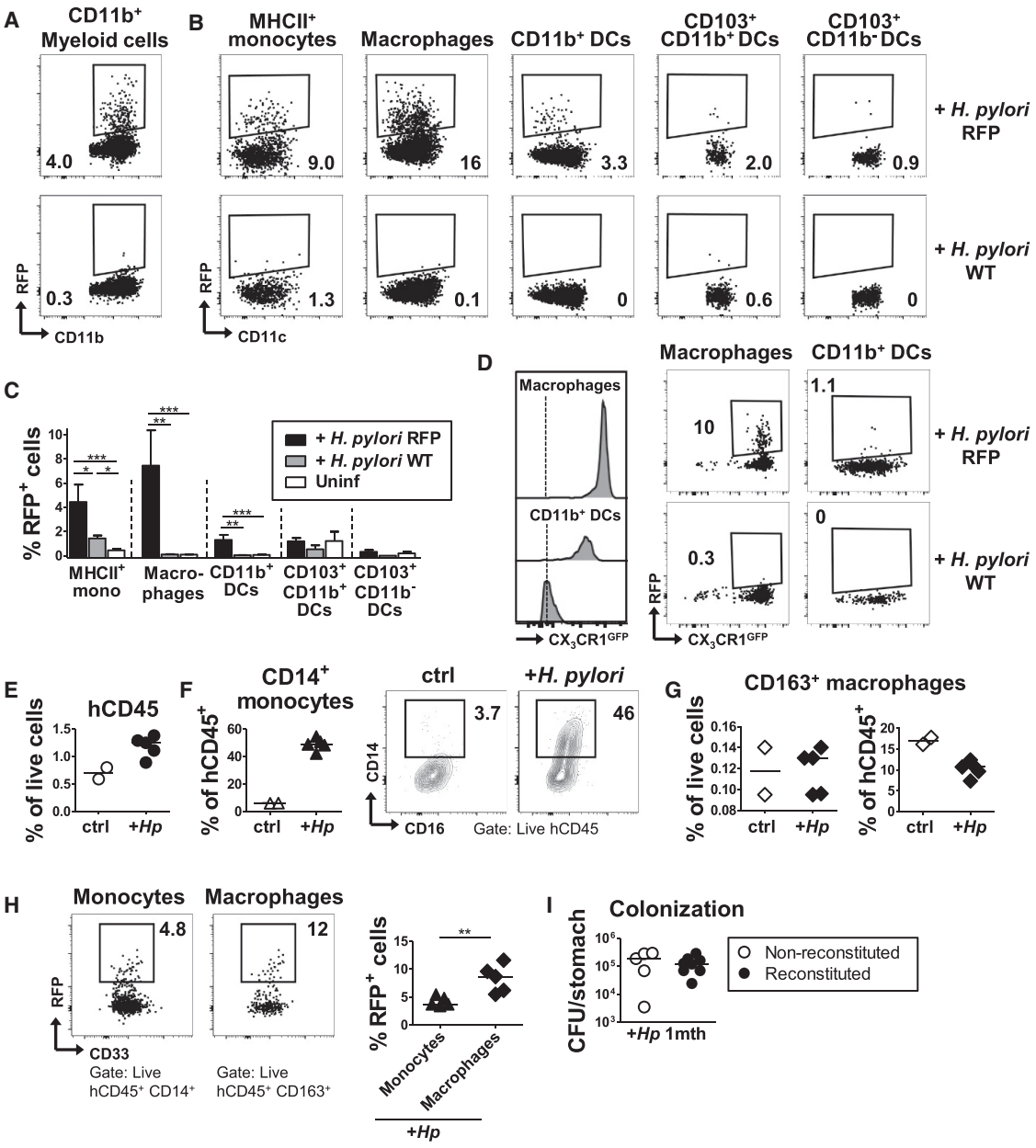

Figure 3. RFP$^+$ *H. pylori* Is Sampled in the Gastric LP by Monocytes, Macrophages, and DCs

(A–D) Mice were infected at 1 week of age with RFP$^+$ or WT (RFP$^-$) *H. pylori* for 3 months prior to the analysis of gastric LP MP populations. Representative FACS plots are shown in (A) and (B).

(A) Frequency of RFP$^+$ cells among all CD11b$^+$ gastric LP myeloid cells.

(B) Frequencies of RFP$^+$ cells among the indicated gastric LP MP populations.

(C) Frequencies of RFP$^+$ cells among the indicated gastric LP MP populations. One representative of 3 independent studies is shown; n = 6–8 mice per group. Data are represented as mean + SEM, and p values were calculated relative to the corresponding uninfected group by Mann-Whitney test.

(D) *CX$_3$CR1*-GFP reporter mice were infected neonatally with RFP$^+$ *H. pylori* or WT *H. pylori*. Frequencies of RFP$^+$ cells among *CX$_3$CR1*-GFP^{hi} gastric LP macrophages and *CX$_3$CR1*-GFP^{dim} CD11b$^+$ DCs are shown in representative FACS plots. The histograms at the left show the *CX$_3$CR1*-GFP expression of the two populations relative to WT (non-transgenic, bottom) cells.

(E–I) MISTRG mice were intrahepatically injected on day 2 of age with 2.5 × 10^5 CD34$^+$ cord blood hematopoietic stem cells and allowed to reconstitute for 6 weeks prior to infection with RFP$^+$ *H. pylori* for 1 month. LP phagocytes were analyzed by flow cytometry. The data shown are representative of 2 independently conducted studies.

(E) Reconstitution efficiency as assessed in the gastric LP.

(F) Frequency of CD14$^+$ monocytes in percent of all human leukocytes in the gastric LP of *H. pylori*-infected relative to uninfected mice. Representative FACS plots are shown at the right.

(legend continued on next page)

responses to mucosal microbes are activated in humanized mice.

TLR2 and NLRP3 Are Upregulated by MPs upon Exposure to *H. pylori*

Because we and others have shown that both the surface-exposed Toll-like receptor TLR2 and the inflammasome sensor NLRP3 are critically involved in detecting *H. pylori* infection in mice and in shaping the adaptive immune response to this infection (Kim et al., 2013; Koch et al., 2015; Semper et al., 2014), we sought to examine the expression and regulation of these factors in gastric LP MP lineages. We first surveyed TLR2 and NLRP3 expression in various MP populations sorted from the gastric LP. Interestingly, the expression patterns of TLR2 and NLRP3 overlapped to a large extent (Figure 4A). Both were expressed strongly in macrophages but not in CD103$^+$ DCs and at an intermediate level in CD11b$^+$ DCs (Figure 4A). TLR2 surface expression on macrophages and CD11b$^+$ DCs could be verified by FACS of LP cells, which further revealed intermediate TLR2 expression on the surface of MHC class II$^-$ monocytes and CD103$^+$CD11b$^+$ DCs and high expression on MHC class II$^+$ monocytes (Figure 4B). *H. pylori* infection increased the fraction of TLR2$^+$ cells among monocytes, macrophages, and CD11b$^+$ DCs but not among CD103$^+$ DCs (Figure 4C). These former populations encounter RFP$^+$ *H. pylori* in the infected mucosa (Figure 3), and so we quantified the mean TLR2 expression on RFP$^+$ and RFP$^-$ fractions of these populations. Interestingly, RFP$^+$ monocytes, macrophages, and CD11b$^+$ DCs showed stronger TLR2 expression than their RFP$^-$ counterparts in the same mice (Figure 4D). Targeted qRT-PCR performed on sorted cell populations confirmed that TLR2 is indeed upregulated transcriptionally in RFP$^+$ macrophages and RFP$^+$ CD11b$^+$ DCs and is part of a signature that comprises NLRP3 and, in DCs, also IL-10 (Figure 4E); the same signature can be detected in sorted macrophages and CD11b$^+$ DCs from infected relative to uninfected mice even when RFP is not used as a marker for sorting (Figure S4). No differences in TLR2 expression were observed upon infection in MP populations of mesenteric lymph nodes (Figure 4F), where TLR2 positivity was also generally much lower, indicating that the expression and upregulation of TLR2 is a feature of tissue-resident populations. We next asked whether TLR2 upregulation could be recapitulated by *H. pylori* exposure of bone marrow-derived DCs (BM-DCs). This was indeed the case (Figure 4G). Furthermore, the approximately 10-fold induction of IL-10 expression in BM-DCs upon *H. pylori* exposure was clearly dependent on TLR2 (Figure 4H). This result extends our earlier observation that IL-10 expression in DCs is required for immune tolerance to *H. pylori* (Engler et al., 2014). The combined results indicate that the monocytes and monocyte-derived macrophages and CD11b$^+$ DCs that encounter *H. pylori* in the infected stomach express TLR2 and NLRP3 already in the steady state and further upregulate both factors upon exposure to *H. pylori*.

NLRP3 Expression Restricts Th1 Responses to *H. pylori* in the Gastric LP

We next sought to examine the role of NLRP3 in MP recruitment to and functionality in the gastric LP. We first examined the MP composition in the LP of NLRP3$^{-/-}$ mice, in the steady state and during infection, relative to wild-type controls. Strikingly, the recruitment of CD11b$^+$ DCs (expressing CD103 or not), but not of monocytes, macrophages, CD103$^+$ DCs, neutrophils, or T cells, to the infected stomach was highly dependent on NLRP3 proficiency of the animals (Figures 5A and S5A). In gastric tissues, both CD11b$^+$ DC populations expressed the transcription factor IRF4 but not IRF8; in contrast, IRF8 expression was detected exclusively in the CD103$^+$ DC lineage (Figure 5B). Wild-type and NLRP3$^{-/-}$ DC populations did not differ with respect to their levels of IRF4 (or IRF8) expression; in particular, the few remaining NLRP3$^{-/-}$ CD11b$^+$ DCs exhibited similar levels of IRF4 expression, as judged by their mean fluorescence intensity (MFI), as their wild-type counterparts (Figure 5B). Consistent with the reported regulatory/anti-inflammatory function of NLRP3 in *H. pylori* infection (Koch et al., 2015), we observed increased gastric Th1 frequencies and gastric mucosal IFN-γ expression in NLRP3$^{-/-}$ relative to wild-type mice, whereas Th17 cell frequencies and IL-17 transcript levels were comparable (Figures 5C and 5D). The strong gastric Th1 responses associated with NLRP3 deficiency were accompanied by lower *H. pylori* colonization levels in the knockout strain (Figure 5E), an inverse association that has been observed previously in wild-type mice (Arnold et al., 2011b; Sayi et al., 2009). Interestingly, Th1 and Th17 frequencies in the MLNs were similar in wild-type and NLRP3$^{-/-}$ mice; although we observed an increase in Th1 frequencies in the MLNs due to infection, indicating that T cell priming in the context of an *H. pylori* infection occurs in these LNs, there were no differences in this regard between wild-type and NLRP3$^{-/-}$ mice (Figure S5B). A similar phenotype was observed with TLR2$^{-/-}$ mice, which also showed increased gastric Th1 frequencies and gastric mucosal IFN-γ expression relative to wild-type mice but comparable Th17 cell frequencies and IL-17 transcript levels (Figures S5C and 5D); the stronger Th1 response again was associated with lower colonization (Figure S5E). As observed in NLRP3$^{-/-}$ mice, Th1 and Th17 frequencies in the MLNs were similar in wild-type and TLR2$^{-/-}$ mice (Figure S5F). The combined results indicate that NLRP3, and also TLR2, functions locally to restrict Th1 responses, which, in turn, limits immune control of the infection.

NLRP3 Controls CD11b$^+$ DC Differentiation in the Gastric LP and in Other GI, Lung, and Lymphoid Tissues in an Inflammasome-Independent Manner

The above results show that the presence of CD11b$^+$ DCs in the *H. pylori*-infected stomach requires NLRP3. To address whether the NLRP3 dependence of CD11b$^+$ DCs holds true not only during infection but also in the steady state and in other GI tissues,

(G) Frequency of CD163$^+$ macrophages in percent of live cells and of human leukocytes in the gastric LP of *H. pylori*-infected relative to uninfected mice.
(H) Frequency of RFP$^+$ cells among CD14$^+$ monocytes and CD163$^+$ macrophages in the gastric LP of *H. pylori*-infected relative to uninfected mice. Representative FACS plots and quantitative data are shown; n = 2–5 mice per group.
(I) *H. pylori* colonization of the mice shown in (E)–(I) as well as of 3 additional reconstituted and 5 un-reconstituted MISTRG mice (n = 5 and 8 mice). Horizontal lines indicate medians. See also Figure S3.

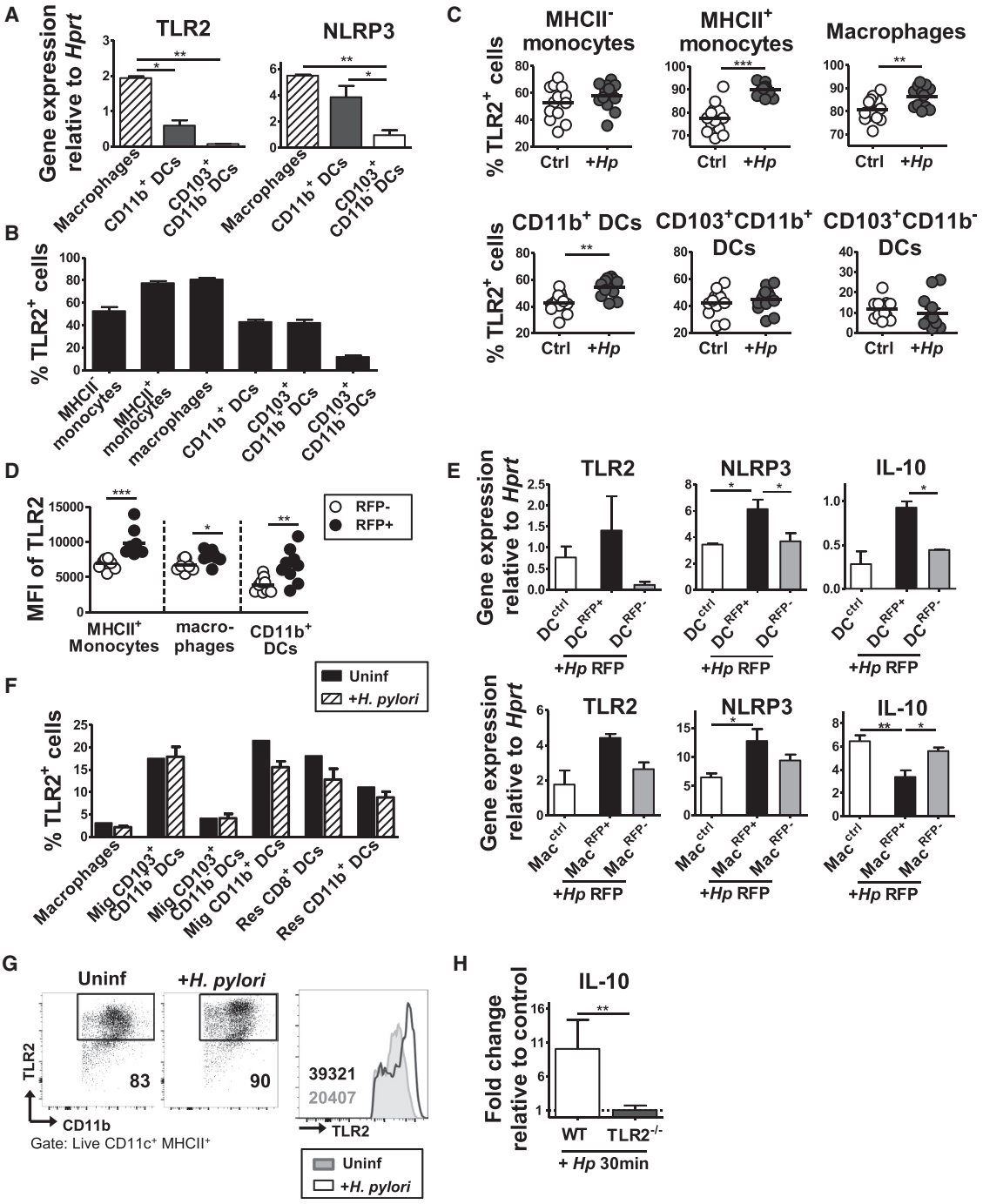

Figure 4. Phagocytes that Encounter *H. pylori* in the Gastric Mucosa Express and Upregulate TLR2 and NLRP3

(A) Expression of TLR2 and NLRP3 by gastric macrophages and CD11b$^+$ and CD103$^+$ DCs, as determined by qRT-PCR of gastric LP populations sorted by FACS and analyzed in 2–4 pools of 1–4 mice. Data are represented as mean + SEM and representative of 2 experiments.

(B) Frequencies of TLR2$^+$ cells among the indicated gastric LP MP populations. Data are represented as mean + SEM of 13 mice (n = 13).

(C) Frequencies of TLR2$^+$ cells among the indicated gastric LP MP populations of *H. pylori*-infected relative to uninfected mice (analyzed 1 month p.i.). Horizontal lines indicate medians. Data are pooled from 3 independent studies (n = 12 and 13).

(D) MFI of TLR2 expression on RFP$^+$ and RFP$^-$ monocytes, macrophages, and CD11b$^+$ DCs. Data are from 1 month-infected mice and pooled from 3 independent studies (n = 8).

(E) Expression of TLR2, NLRP3, and IL-10 by gastric CD11b$^+$ DCs (top) and macrophages (bottom), as determined by qRT-PCR of RFP$^+$ and RFP$^-$ populations sorted by FACS from 2–4 pools of 2–4 mice each. CD11b$^+$ DCs and macrophages from 2 uninfected donors were sorted and analyzed as well. Data are represented as mean + SEM. One representative of 2 independent experiments is shown.

(legend continued on next page)

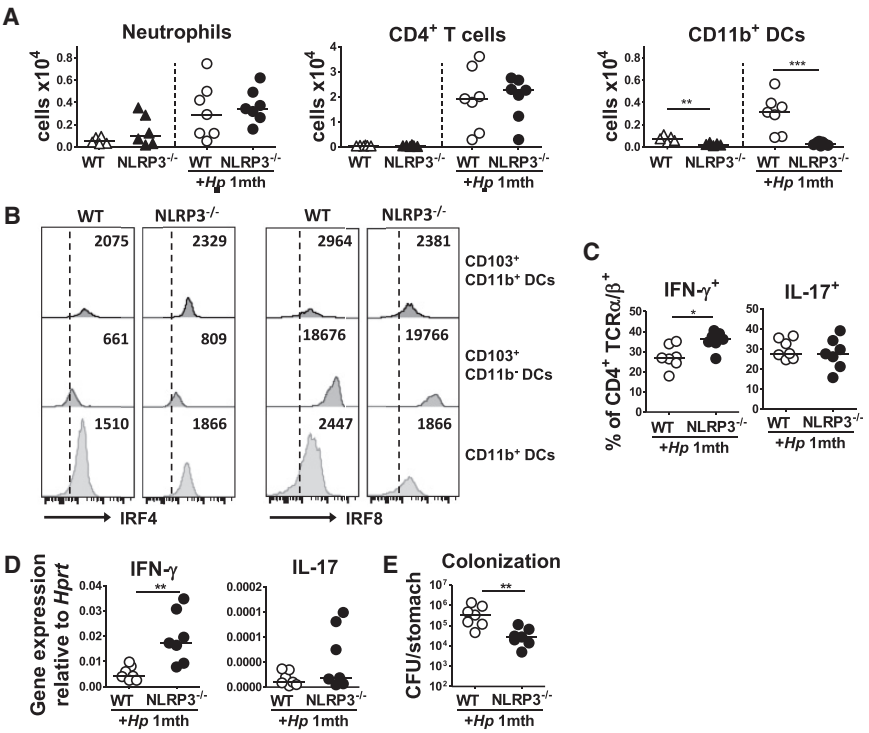

Figure 5. NLRP3 Is Required for the Local Restriction of Th1 Responses to *H. pylori*

NLRP3$^{-/-}$ and wild-type mice were infected with *H. pylori* for 1 month, and their gastric LP leukocytes were analyzed by FACS.

(A) Absolute counts of the indicated gastric LP leukocyte populations in the steady state and at 1 month p.i. with *H. pylori*.

(B) Representative histograms of IRF4 and IRF8 expression of the indicated gastric LP wild-type and NLRP3$^{-/-}$ DC populations. The data as presented are from infected mice. The numbers in the plots indicate the MFI.

(C) Frequencies of IFN-γ$^+$ and IL-17$^+$ cells among all CD4$^+$ T cells of the *H. pylori*-infected mice shown in (A).

(D) IFN-γ and IL-17 expression in the gastric mucosa of the *H. pylori*-infected mice shown in (A) and (C), as determined by qRT-PCR.

(E) *H. pylori* colonization of the mice shown in (A), (C), and (D). The data in (A) and (C)–(E) are from one study that is representative of 4 independent ones; n = 5–7 mice per group.

*p < 0.05, **p < 0.01, ***p < 0.001, as calculated by Mann-Whitney test. See also Figure S5.

we compared the frequencies of CD11b$^+$ DCs (Figure 6A) and of other DC subsets and macrophages (Figure S6A) in the LP of the stomach, SI and colon. Interestingly, although all other examined cell types were present at normal frequencies, CD11b$^+$ DCs were absent in all GI tissues of NLRP3$^{-/-}$ mice in the steady state. The same dependency of CD11b$^+$ DCs on NLRP3 was observed in lung tissues and, for their counterpart populations, in the MLNs (Figure S6A). To address whether the NLRP3 dependency of CD11b$^+$ DCs reflects their concomitant reliance on microbial NLRP3 activation, we treated both wild-type and NLRP3$^{-/-}$ mice with the antibiotics ampicillin, neomycin, metronidazole, and vancomycin to remove the bulk of microbial sources of NLRP3 activation. This treatment failed to reduce CD11b$^+$ DC frequencies in the colons of wild-type mice to NLRP3$^{-/-}$ levels (Figure S6B), suggesting that non-microbial NLRP3 activation may be more important than microbial NLRP3 ligands in promoting the differentiation and/or recruitment of CD11b$^+$ DCs. To address whether the NLRP3 dependence of CD11b$^+$ DC differentiation is cell-intrinsic, we generated bone marrow chimeras in which NLRP3-proficient and -deficient cells were analyzed in the same environment. Interestingly, NLRP3 was clearly required in a cell-intrinsic manner in CD11b$^+$ DCs for their differentiation in the gastric mucosa (Figures 6B and 6C). NLRP3 is predominantly known for its function as an inflammasome component that interacts with caspase-1 and the adaptor molecule apoptosis-associated speck-like protein containing a carboxy-terminal CARD (ASC) to form multimeric inflammasomes; in the context of *Helicobacter* infections, NLRP3 (but not NLRC4, AIM2, or NLRP6) contribute to caspase-1 activation and proIL-1β/proIL-18 processing (Hitzler et al., 2012; Koch et al., 2015). We therefore tested how the inflammasome components caspase-1 and ASC and the caspase-1-dependent cytokine IL-18 contribute to CD11b$^+$ DC frequencies in the steady state by assessing the gastric CD11b$^+$ DC compartment of the respective knockout mice. Interestingly, the CD11b$^+$ DC deficiency of NLRP3$^{-/-}$ mice was not shared by caspase-1$^{-/-}$ or ASC$^{-/-}$ mice and was also not observed in mice lacking the receptor for the caspase-1-dependent cytokine IL-18 (Figure 6D). To address whether the dependence of CD11b$^+$ DCs on NLRP3 expression could be recapitulated in a simple *in vitro* culture of DCs from bone marrow precursors, we quantified the frequencies of CD11b$^+$ DCs, macrophages, and CD103$^+$ DCs in wild-type and NLRP3$^{-/-}$ bone marrow cultures that were exposed to FLT3 ligand for 10 days. Although culturing of wild-type bone marrow cells with FLT3 ligand gave rise to a clearly discernible population of CD11b$^+$ DCs, this population was strongly reduced in NLRP3$^{-/-}$ cultures (Figures 6E and S7A). NLRP3 deficiency rather favored the development of

(F) Frequencies of TLR2$^+$ cells among the indicated MLN macrophage and DC populations of 7 *H. pylori*-infected relative to 2 uninfected mice. Data are represented as mean + SEM. mig, migratory; res, resident.

(G) Bone marrow (BM)-derived DCs differentiated with GM-CSF were infected with *H. pylori* at an MOI of 50 for 24 hr prior to staining for TLR2 expression.

(H) WT and TLR2$^{-/-}$ BM-DCs were infected with *H. pylori* for 30 min prior to qRT-PCR analysis of IL-10 expression. Data are represented as mean + SEM of 3 independent experiments (n = 3 experiments).

*p < 0.05, **p < 0.01, ***p < 0.001, as calculated by Mann-Whitney test (C, D, and H) or one-way ANOVA with Tukey's post-test (A and E). See also Figure S4.

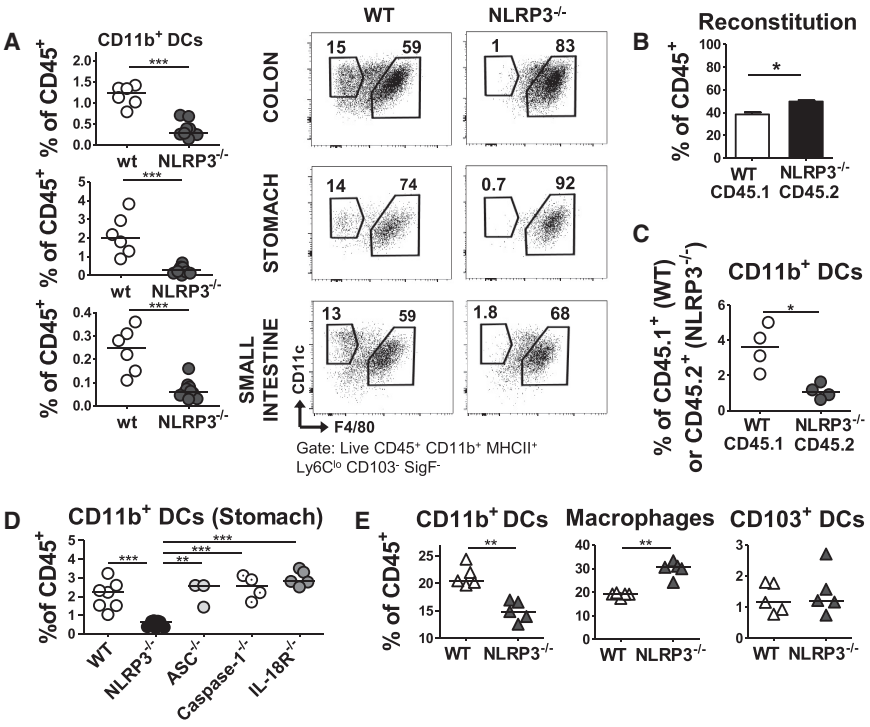

Figure 6. NLRP3 Is Required for the Differentiation or Recruitment of CD11b$^+$ DCs in/to GI Tissues

(A) Frequencies of CD11b$^+$ DCs among CD45$^+$ cells in the LP of the colon, stomach, and SI of WT and NLRP3$^{-/-}$ mice. Representative FACS plots are shown on the right. Data are pooled from 2 experiments (n = 6–10 mice per group).

(B and C) Adult WT mice were reconstituted with 1:1 mixed BM from CD45.1$^+$ WT and CD45.2$^+$ NLRP3$^{-/-}$ donors. Mice were allowed to reconstitute for 6 weeks prior to a 6-week infection with *H. pylori*. The reconstitution efficiency is shown in (B). The frequencies of CD11b$^+$ DCs are shown in (C). Data are from a single experiment.

(D) Frequencies of CD11b$^+$ DCs among CD45$^+$ cells in the gastric LP of WT, NLRP3$^{-/-}$, ASC$^{-/-}$, caspase-1$^{-/-}$, and IL18R$^{-/-}$ mice.

(E) WT and NLRP3$^{-/-}$ BM cells were differentiated with FLT3L for 9 days. Frequencies of CD11b$^+$ DCs, macrophages, and CD103$^+$ DCs as percent of live leukocytes. Data are pooled from three independent experiments.

$^*p < 0.05$, $^{**}p < 0.01$, $^{***}p < 0.001$, as calculated by Mann-Whitney test (A–C and E) or one-way ANOVA with Tukey's post-test (D). See also Figures S6 and S7.

macrophages, whereas CD103$^+$ DCs constituted a minor but similarly sized population in both cultures (Figure 6E). Because CD11b$^+$ DCs are known to depend on the transcription factor IRF4 (Scott et al., 2015), we examined the expression of IRF4 and of two other DC-specific transcription factors—BATF3 and Zbtb46—in our FLT3L-derived cultures. Strikingly, only the expression of IRF4, but not of the other two transcription factors, was reduced in NLRP3$^{-/-}$ relative to wild-type cultures (Figure S7B), reflecting the loss of CD11b$^+$ DCs. IRF4 staining or FACS-sorting of CD11b$^+$ DCs followed by IRF4-specific qRT-PCR revealed, however, that the residual CD11b$^+$ DC population found in NLRP3$^{-/-}$ cultures did not differ from their wild-type counterparts with respect to IRF4 expression (Figure S7C and data not shown). The combined results suggest that NLRP3 has a cell-intrinsic, inflammasome-independent function in driving the differentiation of CD11b$^+$ DCs in GI, lung, and lymphoid tissues in both the steady state and during infection. This non-canonical function of NLRP3 cannot be attributed to a direct regulation of the lineage-defining transcription factor IRF4 by NLRP3.

NLRP3 Is Required for the Recruitment or Expansion of Both Thymus-Derived and Peripherally Induced Regulatory T Cells

NLRP3$^{-/-}$ mice exhibit excessive local Th1 responses that likely account for their more efficient control of *H. pylori* infections relative to wild-type animals. To address whether the deregulated Th1 response is due to the inability of the animals to generate a proper regulatory T cell (Treg) response, we analyzed the gastric and MLN Treg compartment in infected relative to naive mice of both genotypes. Interestingly, we observed robust recruitment to and/or expansion of CD4$^+$Foxp3$^+$ Tregs in the infected relative to the naive gastric mucosa (Figures 7A and 7B). The accumulation of Foxp3$^+$ Tregs was significantly reduced in NLRP3$^{-/-}$ mice (Figures 7A and 7B). Interestingly, both neuropilin-negative peripherally-induced regulatory T cells (pTregs) and neuropilin-positive thymus-derived regulatory T cells (tTregs) accumulated in the infected stomach, and both subsets were reduced due to NLRP3 deficiency (Figure 7C). In contrast, Foxp3$^+$ Treg frequencies in the MLNs did not change as a result of infection or due to NLRP3 deficiency (Figure S7D). Neither pTreg nor tTreg frequencies changed much in the MLNs of wild-type mice due to infection (Figure S7E); in contrast, pTreg to tTreg ratios were shifted in NLRP3$^{-/-}$ mice in favor of tTregs, indicating that pTreg priming in LNs may require NLRP3 or NLRP3-dependent DC lineages. The combined results suggest that colonization of the gastric mucosa by *H. pylori* results in local accumulation of both natural and peripherally induced Treg subsets and that this accumulation (recruitment or local expansion) depends on NLRP3.

DISCUSSION

Our comparative analysis of MP evolution in early life revealed the stomach to be a predominantly myeloid organ with little or no lymphocyte contribution to the overall leukocyte population; this was in sharp contrast to both the small and large intestine, where lymphocytes represent the dominant immune cell compartments. The neonatal stomach is special in that it is populated by MP subsets that disappear later in life, at least in the steady state; MHC class II-negative monocytes/macrophages, CD103$^+$ cDC1s, and CD11b$^+$ cDC2s are all initially present on

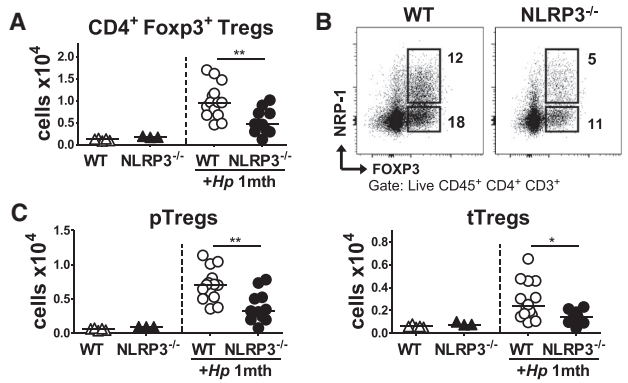

Figure 7. NLRP3 Is Required for Regulatory T Cell Responses to *H. pylori* Infection

(A–C) NLRP3$^{-/-}$ and WT mice were infected with *H. pylori* for 1 month and their gastric LP Treg compartment was analyzed by FACS.

(A) Absolute counts of Foxp3^{+} CD4^{+} Tregs in the gastric LP of WT and NLRP3$^{-/-}$ mice in the steady state and at 1 month p.i. with *H. pylori*.

(B) Representative FACS plots showing the reduction of gastric neuropilin-1-negative (NRP-1^{-}) Foxp3^{+} peripherally induced pTregs and of NRP-1^{+} Foxp3^{+} thymus-derived tTregs in a NLRP3$^{-/-}$ relative to a WT mouse.

(C) Absolute counts of pTregs and tTregs in the gastric LP of the WT and NLRP3$^{-/-}$ mice shown in (A).

The data in (A) and (C) are pooled from 2 independent experiments (n = 3–14 mice per group). *p < 0.05, **p < 0.01, ***p < 0.001, as calculated by Mann-Whitney test. See also Figure S7.

day 7 and gradually decline within the first 2–4 weeks of life. The dramatic loss of entire populations is not observed in the SI, which shows more or less gradual increases in all MP populations as well as in overall cellularity. Upon infection with *H. pylori*, the composition of the gastric LP changes profoundly, with a robust but numerically modest increase observed in all three DC subsets as well as monocytes and macrophages and a numerically much more striking increase observed in neutrophils and CD4^{+} T cells. Virtually all infiltrating T cells are activated and polarized to produce Th1 and/or Th17 cytokines; this is in contrast to the naive stomach, where T cells are extremely scarce. As reported previously (Arnold et al., 2011b), only exposure of adult mice results in strong T cell infiltration and a concomitant control of the infection; in contrast, neonatal exposure fails to attract T cells (even as infected mice age), explaining why neonatally infected mice sustain high levels of *H. pylori* colonization for life (Arnold et al., 2011b). In the neonatal stomach, *H. pylori* is faced with specific DC and MHC class II^{-} macrophage/monocyte populations that are not present at high numbers in the adult stomach; the differences in the dominant APC populations at the time of the first encounter may account for the differences in T cell recruitment and polarization.

The increase in MP numbers in the infected gastric mucosa is highly dependent on CCR2; bone marrow chimera experiments revealed, however, that only certain lineages (monocytes, macrophages, and CD11b^{+} DCs) cell-intrinsically require CCR2 signaling for their tissue recruitment. *Bona fide* DC populations (CD103^{+} CD11b^{+} and CD103^{+} CD11b^{-}) are present in normal numbers in the infected mucosa even when they lack CCR2. This finding is in agreement with previous reports showing that Ly6C^{hi}CCR2^{+} monocytes give rise to macrophages and Cx_3CR1^{dim} CD11b^{+} MPs in both the healthy and inflamed colon in a process that involves downregulation of Ly6C and upregulation of MHC class II, CD11c, CX_3CR1, and (in macrophages) F4/80 and CD64 (Bain et al., 2013), whereas the two CD103^{+} DC subsets arise from Flt3L-dependent pre-DC progenitors that neither express nor require CCR2 (Bogunovic et al., 2009; Varol et al., 2009). Bain et al. (2013) further raise the intriguing possibility that Cx_3CR1^{dim} CD11b^{+} MPs represent an intermediate cell type in arrested development under conditions of inflammation. This view is challenged by genetic tracing experiments linking CD11b^{+} DCs to a pre-DC progenitor (Schraml et al., 2013); more recent evidence confirmed that intestinal CD11b^{+} MPs are indeed classical DCs derived from Flt3 ligand-dependent, DC-committed precursors despite the fact that a large fraction of these cells express CCR2 (Scott et al., 2015). Our data indicate that CX_3CR1^{dim} CD11b^{+} MPs, which are very abundant in the *H. pylori*-infected mucosa, exhibit properties of both DCs and macrophages; they are largely absent in Flt3L-deficient mice but share many surface receptors (CX_3CR1, TLR2) and the cell-intrinsic developmental CCR2 requirement with macrophages.

The generation of RFP-expressing bacteria allowed us to address which MP populations encounter *H. pylori* in the infected mucosa. To our surprise, we found that MHC class II^{+} monocytes, macrophages, and CD11b^{+} DCs, but not CD103^{+} DC lineages, showed evidence of recent *H. pylori* encounters. The bacterially derived RFP signal further allowed us to study the consequences of *H. pylori* contact for MP gene expression by comparison of transcripts between RFP-positive and -negative fractions of MP populations harvested from the same stomach. Not surprisingly, we found the anti-inflammatory cytokine IL-10 to be induced in CD11b^{+} DCs upon *H. pylori* contact; this finding is in agreement with our previous observation that DC-intrinsic production of IL-10 (which we examined in *CD11c*-Cre x IL-10$^{fl/fl}$ mice) is required for *H. pylori*-induced immune tolerance and protection against allergic asthma, which is a hallmark of neonatally infected mice (Engler et al., 2014).

Quite unexpectedly, we found NLRP3 to be cell-intrinsically required for the local differentiation of CD11b^{+} DCs not only in the stomach but throughout the GI tract, lung, and lymphoid tissues in both the steady state and during infection. This property of NLRP3 appears to be unrelated to its role as a cytoplasmic sensor and trigger of inflammasome activation because neither caspase-1$^{-/-}$ nor ASC$^{-/-}$ mice share the CD11b^{+} deficiency of NLRP3$^{-/-}$ mice. Interestingly, the requirement of NLRP3 for CD11b^{+} DC differentiation could be recapitulated in FLT3 ligand-derived DC cultures from bone marrow. We confirmed previous results indicating that IRF4 expression is high in CD11b^{+} and CD103^{+} CD11b^{+} DCs (cDC2s) and low in CD103^{+} DCs (cDC1s) (Scott et al., 2015), which is mirrored by the differential dependence of these subsets on NLRP3 expression shown here. Interestingly, NLRP3 and IRF4 have been reported to physically interact in the nucleus of T cells, where they bind to the *Il4* promoter to activate IL-4 transcription, driving Th2 differentiation in a T cell-intrinsic manner (Bruchard et al., 2015). Our preliminary data using co-immunoprecipitation and chromatin immunoprecipitation (ChIP)

(data not shown), and also qRT-PCRs of *in vitro* cultures, currently do not support a model in which NLRP3 and IRF4 interact directly in myeloid cells and also do not suggest a role for NLRP3 as a transcription factor regulating IRF4 expression directly; more work is clearly required to shed light on the NLRP3-dependent signals governing CD11b^{+} DC development. In summary, we show here that the gastric LP is populated by a complex network of MPs in the steady state and especially during infection, which orchestrates a fine balance of maintaining tissue homeostasis while effectively controlling invading pathogens.

EXPERIMENTAL PROCEDURES

Mice

C57BL/6 wild-type (WT), B6.SJL-Cd45.1, Tlr2$^{-/-}$, Nlrp3$^{-/-}$, *Ccr2*$^{-/-}$, and CX$_3$CR1$^{GFP/+}$ mice were obtained from The Jackson Laboratory. ASC$^{-/-}$, caspase-1$^{-/-}$, IL-18R$^{-/-}$, and MISTRG mice have all been described previously (Koch et al., 2015; Oertli et al., 2012; Rongvaux et al., 2014). All strains were bred and maintained under specific pathogen-free conditions in accredited animal facilities at the University of Zürich. All animal experiments were reviewed and approved by the Zürich Cantonal Veterinary Office (licenses ZH170/2014, ZH24/2013, and ZH235/2015 to A.M.). The generation of bone marrow chimeras, reconstitution of humanized mice, and antibiotic treatment regimens are described in the Supplemental Experimental Procedures, along with protocols for ILP leukocyte isolation and bone marrow-derived cell cultures.

H. pylori Infection

Mice of both genders were infected orally on 2 consecutive days with 10^8 colony-forming units (CFUs) *H. pylori* PMSS1 at 6 weeks or 7 days of age and analyzed at 1 and 3 months p.i. unless specified otherwise. *H. pylori* strains, culture conditions, and colony counting are described in the Supplemental Experimental Procedures.

Statistical Analysis

Statistical analysis was performed with Prism 6.0 (GraphPad). The nonparametric Mann-Whitney test was used for most statistical comparisons conducted on *in vivo* data because it does not require the assumption of normal distribution. The one-way ANOVA test was used to compare three or more sets of measurements. Tukey's multiple comparisons post-test was used to compare all pairs of means of three or more datasets unless otherwise specified; in general, the applied statistical tests are listed in all figure legends. Differences were considered statistically significant when $p < 0.05$ (*$p < 0.05$, **$p < 0.01$, ***$p < 0.001$).

SUPPLEMENTAL INFORMATION

Supplemental Information includes Supplemental Experimental Procedures and seven figures and can be found with this article online at https://doi.org/10.1016/j.celrep.2017.12.015.

ACKNOWLEDGMENTS

This work was supported by Swiss National Science Foundation Temporary Backup Schemes Consolidator Grant BSCGIO_157841/1 (to A.M.) and the Clinical Research Priority Program on Human Hemato-Lymphatic Diseases, University of Zurich. We thank Melanie Greter and Maries van den Broek for helpful discussions. We are grateful to Lubor Borsig for sharing CCR2$^{-/-}$ mice and to the technical staff of the Department of Hematology for preparing human cord blood HSCs.

AUTHOR CONTRIBUTIONS

I.C.A. designed, performed, and analyzed most of the experiments and cowrote the manuscript. S.U. and X.Z. contributed several *in vivo* experiments and performed BM-DC infections. M.A.-B. performed qPCRs. M.G.M. and K.M.O. provided critical tools and intellectual input. A.M. supervised the studies and co-wrote the manuscript.

DECLARATION OF INTERESTS

The authors declare no competing interests.

Received: May 24, 2017
Revised: October 24, 2017
Accepted: December 1, 2017
Published: December 26, 2017

REFERENCES

Arnold, I.C., Dehzad, N., Reuter, S., Martin, H., Becher, B., Taube, C., and Müller, A. (2011a). Helicobacter pylori infection prevents allergic asthma in mouse models through the induction of regulatory T cells. J. Clin. Invest. *121*, 3088–3093.

Arnold, I.C., Lee, J.Y., Amieva, M.R., Roers, A., Flavell, R.A., Sparwasser, T., and Müller, A. (2011b). Tolerance rather than immunity protects from Helicobacter pylori-induced gastric preneoplasia. Gastroenterology *140*, 199–209.

Bain, C.C., Scott, C.L., Uronen-Hansson, H., Gudjonsson, S., Jansson, O., Grip, O., Guilliams, M., Malissen, B., Agace, W.W., and Mowat, A.M. (2013). Resident and pro-inflammatory macrophages in the colon represent alternative context-dependent fates of the same Ly6Chi monocyte precursors. Mucosal Immunol. *6*, 498–510.

Blaser, M.J., Chen, Y., and Reibman, J. (2008). Does Helicobacter pylori protect against asthma and allergy? Gut *57*, 561–567.

Bogunovic, M., Ginhoux, F., Helft, J., Shang, L., Hashimoto, D., Greter, M., Liu, K., Jakubzick, C., Ingersoll, M.A., Leboeuf, M., et al. (2009). Origin of the lamina propria dendritic cell network. Immunity *31*, 513–525.

Bruchard, M., Rebé, C., Derangère, V., Togbé, D., Ryffel, B., Boidot, R., Humblin, E., Hamman, A., Chalmin, F., Berger, H., et al. (2015). The receptor NLRP3 is a transcriptional regulator of TH2 differentiation. Nat. Immunol. *16*, 859–870.

Castano-Rodriguez, N., Kaakoush, N.O., Lee, W.S., and Mitchell, H.M. (2017). Dual role of Helicobacter and Campylobacter species in IBD: a systematic review and meta-analysis. Gut *66*, 235–249.

Cerovic, V., Houston, S.A., Scott, C.L., Aumeunier, A., Yrlid, U., Mowat, A.M., and Milling, S.W. (2013). Intestinal CD103(-) dendritic cells migrate in lymph and prime effector T cells. Mucosal Immunol. *6*, 104–113.

Cerovic, V., Bain, C.C., Mowat, A.M., and Milling, S.W. (2014). Intestinal macrophages and dendritic cells: what's the difference? Trends Immunol. *35*, 270–277.

Edelson, B.T., Kc, W., Juang, R., Kohyama, M., Benoit, L.A., Klekotka, P.A., Moon, C., Albring, J.C., Ise, W., Michael, D.G., et al. (2010). Peripheral CD103+ dendritic cells form a unified subset developmentally related to CD8alpha+ conventional dendritic cells. J. Exp. Med. *207*, 823–836.

Engler, D.B., Reuter, S., van Wijck, Y., Urban, S., Kyburz, A., Maxeiner, J., Martin, H., Yogev, N., Waisman, A., Gerhard, M., et al. (2014). Effective treatment of allergic airway inflammation with Helicobacter pylori immunomodulators requires BATF3-dependent dendritic cells and IL-10. Proc. Natl. Acad. Sci. USA *111*, 11810–11815.

Engler, D.B., Leonardi, I., Hartung, M.L., Kyburz, A., Spath, S., Becher, B., Rogler, G., and Müller, A. (2015). Helicobacter pylori-specific protection against inflammatory bowel disease requires the NLRP3 inflammasome and IL-18. Inflamm. Bowel Dis. *21*, 854–861.

Greter, M., Helft, J., Chow, A., Hashimoto, D., Mortha, A., Agudo-Cantero, J., Bogunovic, M., Gautier, E.L., Miller, J., Leboeuf, M., et al. (2012). GM-CSF controls nonlymphoid tissue dendritic cell homeostasis but is dispensable for the differentiation of inflammatory dendritic cells. Immunity *36*, 1031–1046.

Haniffa, M., Shin, A., Bigley, V., McGovern, N., Teo, P., See, P., Wasan, P.S., Wang, X.N., Malinarich, F., Malleret, B., et al. (2012). Human

tissues contain CD141hi cross-presenting dendritic cells with functional homology to mouse CD103+ nonlymphoid dendritic cells. Immunity *37*, 60–73.

Harris, P.R., Wright, S.W., Serrano, C., Riera, F., Duarte, I., Torres, J., Peña, A., Rollán, A., Viviani, P., Guiraldes, E., et al. (2008). Helicobacter pylori gastritis in children is associated with a regulatory T-cell response. Gastroenterology *134*, 491–499.

Hitzler, I., Sayi, A., Kohler, E., Engler, D.B., Koch, K.N., Hardt, W.D., and Müller, A. (2012). Caspase-1 has both proinflammatory and regulatory properties in Helicobacter infections, which are differentially mediated by its substrates IL-1β and IL-18. J. Immunol. *188*, 3594–3602.

Kim, D.J., Park, J.H., Franchi, L., Backert, S., and Núñez, G. (2013). The Cag pathogenicity island and interaction between TLR2/NOD2 and NLRP3 regulate IL-1β production in Helicobacter pylori infected dendritic cells. Eur. J. Immunol. *43*, 2650–2658.

Kingston, D., Schmid, M.A., Onai, N., Obata-Onai, A., Baumjohann, D., and Manz, M.G. (2009). The concerted action of GM-CSF and Flt3-ligand on in vivo dendritic cell homeostasis. Blood *114*, 835–843.

Koch, K.N., Hartung, M.L., Urban, S., Kyburz, A., Bahlmann, A.S., Lind, J., Backert, S., Taube, C., and Müller, A. (2015). Helicobacter urease-induced activation of the TLR2/NLRP3/IL-18 axis protects against asthma. J. Clin. Invest. *125*, 3297–3302.

Lavin, Y., Mortha, A., Rahman, A., and Merad, M. (2015). Regulation of macrophage development and function in peripheral tissues. Nat. Rev. Immunol. *15*, 731–744.

Lewis, K.L., Caton, M.L., Bogunovic, M., Greter, M., Grajkowska, L.T., Ng, D., Klinakis, A., Charo, I.F., Jung, S., Gommerman, J.L., et al. (2011). Notch2 receptor signaling controls functional differentiation of dendritic cells in the spleen and intestine. Immunity *35*, 780–791.

Mowat, A.M., and Agace, W.W. (2014). Regional specialization within the intestinal immune system. Nat. Rev. Immunol. *14*, 667–685.

Oertli, M., Sundquist, M., Hitzler, I., Engler, D.B., Arnold, I.C., Reuter, S., Maxeiner, J., Hansson, M., Taube, C., Quiding-Järbrink, M., and Müller, A. (2012). DC-derived IL-18 drives Treg differentiation, murine Helicobacter pylori-specific immune tolerance, and asthma protection. J. Clin. Invest. *122*, 1082–1096.

Oertli, M., Noben, M., Engler, D.B., Semper, R.P., Reuter, S., Maxeiner, J., Gerhard, M., Taube, C., and Müller, A. (2013). Helicobacter pylori γ-glutamyl transpeptidase and vacuolating cytotoxin promote gastric persistence and immune tolerance. Proc. Natl. Acad. Sci. USA *110*, 3047–3052.

Persson, E.K., Uronen-Hansson, H., Semmrich, M., Rivollier, A., Hägerbrand, K., Marsal, J., Gudjonsson, S., Håkansson, U., Reizis, B., Kotarsky, K., and Agace, W.W. (2013). IRF4 transcription-factor-dependent CD103(+) CD11b(+) dendritic cells drive mucosal T helper 17 cell differentiation. Immunity *38*, 958–969.

Rongvaux, A., Willinger, T., Martinek, J., Strowig, T., Gearty, S.V., Teichmann, L.L., Saito, Y., Marches, F., Halene, S., Palucka, A.K., et al. (2014). Development and function of human innate immune cells in a humanized mouse model. Nat. Biotechnol. *32*, 364–372.

Salama, N.R., Hartung, M.L., and Müller, A. (2013). Life in the human stomach: persistence strategies of the bacterial pathogen Helicobacter pylori. Nat. Rev. Microbiol. *11*, 385–399.

Sayi, A., Kohler, E., Hitzler, I., Arnold, I., Schwendener, R., Rehrauer, H., and Müller, A. (2009). The CD4+ T cell-mediated IFN-gamma response to Helicobacter infection is essential for clearance and determines gastric cancer risk. J. Immunol. *182*, 7085–7101.

Schraml, B.U., van Blijswijk, J., Zelenay, S., Whitney, P.G., Filby, A., Acton, S.E., Rogers, N.C., Moncaut, N., Carvajal, J.J., and Reis e Sousa, C. (2013). Genetic tracing via DNGR-1 expression history defines dendritic cells as a hematopoietic lineage. Cell *154*, 843–858.

Scott, C.L., Bain, C.C., Wright, P.B., Sichien, D., Kotarsky, K., Persson, E.K., Luda, K., Guilliams, M., Lambrecht, B.N., Agace, W.W., et al. (2015). CCR2(+)CD103(-) intestinal dendritic cells develop from DC-committed precursors and induce interleukin-17 production by T cells. Mucosal Immunol. *8*, 327–339.

Semper, R.P., Mejías-Luque, R., Groß, C., Anderl, F., Müller, A., Vieth, M., Busch, D.H., Prazeres da Costa, C., Ruland, J., Groß, O., and Gerhard, M. (2014). Helicobacter pylori-induced IL-1β secretion in innate immune cells is regulated by the NLRP3 inflammasome and requires the cag pathogenicity island. J. Immunol. *193*, 3566–3576.

Varol, C., Vallon-Eberhard, A., Elinav, E., Aychek, T., Shapira, Y., Luche, H., Fehling, H.J., Hardt, W.D., Shakhar, G., and Jung, S. (2009). Intestinal lamina propria dendritic cell subsets have different origin and functions. Immunity *31*, 502–512.

Zhou, X., Wu, J., and Zhang, G. (2013). Association between Helicobacter pylori and asthma: a meta-analysis. Eur. J. Gastroenterol. Hepatol. *25*, 460–468.